Bioorganic & Medicinal Chemistry 24 (2016) 1919–1926

Contents lists available at ScienceDirect

Bioorganic & Medicinal Chemistry

journal homepage: www.elsevier.com/locate/bmc

Discovery of new low-molecular-weight p53–Mdmx disruptors and their anti-cancer activities

Shinichi Uesato [a,*], Yoshihiro Matsuura [a], Saki Matsue [a], Takaaki Sumiyoshi [a], Yoshiyuki Hirata [a], Suzuho Takemoto [a], Yasuyuki Kawaratani [a], Yusuke Yamai [a], Kyoji Ishida [a], Tsutomu Sasaki [b], Masato Enari [c,*]

[a] Department of Life Science and Biotechnology, Faculty of Chemistry, Materials and Bioengineering, Kansai University, Suita, Osaka 564-8680, Japan
[b] Department of Neurology, Graduate School of Medicine, Osaka University, Yamadaoka 2-2, Suita, Osaka 565-0871, Japan
[c] Division of Refractory and Advanced Cancer, National Cancer Center Research Institute, Chuo-ku, Tokyo 104-0045, Japan

ARTICLE INFO

Article history:
Received 11 February 2016
Revised 8 March 2016
Accepted 10 March 2016
Available online 11 March 2016

Keywords:
o-Aminothiophenol derivative
p53–Mdmx-interaction inhibitor
Protein–protein interaction inhibitor
Modified ELISA
GST–Mdmx

ABSTRACT

Although several p53–Mdm2-binding disruptors have been identified to date, few studies have been published on p53–Mdmx-interaction inhibitors. In the present study, we demonstrated that *o*-aminothiophenol derivatives with molecular weights of 200–300 selectively inhibited the p53–Mdmx interaction. *S*-2-Isobutyramidophenyl 2-methylpropanethioate (K-178) (**1c**) activated p53, up-regulated the expression of its downstream genes such as p21 and Mdm2, and preferentially inhibited the growth of cancer cells with wild-type p53 over those with mutant p53. Furthermore, we found that the *S*-isobutyryl-deprotected forms **1b** and **3b** of **1c** and *S*-2-benzamidophenyl 2-methylpropanethioate (K-181) (**3c**) preferentially inhibited the p53–Mdmx interaction over the p53–Mdm2 interaction, respectively, by using a Flag-p53 and glutathione S-transferase (GST)-fused protein complex (Mdm2, Mdmx, DAPK1, or PPID). In addition, the interaction of p53 with Mdmx was lost by replacing a sulfur atom with an oxygen atom in **1b** and **1c**. These results suggest that sulfides such as **1b**, **3b**, **4b**, and **5b** interfere with the binding of p53–Mdmx, resulting in the dissociation of the two proteins. Furthermore, the results of oral administration experiments using xenografts in nude mice indicated that **1c** reduced the volume of tumor masses to 49.0% and 36.6% that of the control at 100 mg/kg and 150 mg/kg, respectively, in 40 days.

1. Introduction

The tumor suppressor p53 induces cell cycle arrest and apoptosis in response to cellular stresses by activating the expression of its downstream genes.[1–5] However, in some cancer cells, negative regulators such as Mdm2, Mdmx, COP1, Pirh2, Arf-BP1, and synoviolin impair the functions of p53.[6–8] For example, Mdm2 exhibits E3 ubiquitin ligase activity and inactivates the functions of p53 via the ubiquitin–proteasome system. In contrast, Mdmx, a homolog of Mdm2, has no ubiquitin ligase activity to conjugate ubiquitin with p53.[9] Mdmx interacts with Mdm2 to enhance ubiquitination of p53 and ubiquitinated p53 degrades via the proteasome system to inhibit p53 function. In addition to the degradation pathway, the Mdm2–Mdmx complex is known as a factor in the nuclear export of p53 through its mono-ubiquitination to inactivate p53-mediated transcription.[8,10] Mdm2 and Mdmx both bind to p53 through hydrophobic interactions as follows. p53 forms a short helix inside the p53-binding cleft of Mdm2 or Mdmx, and the three residues: Phe19, Trp23, and Leu26, of the helix principally contribute to binding to Mdm2 or Mdmx. A large number of p53–Mdm2-binding disruptors have been identified to date.[11–15] For example, Nutlin-3a is a useful compound that inhibits the p53–Mdm2 interaction by docking antagonistically in the p53-binding domain of Mdm2.[16] On the other hand, Nutlin-3a is less likely to inhibit p53–Mdmx binding,[17] and this may be interpreted in terms of differences in the sizes of the p-53 binding sites of Mdm2 and Mdmx as follows. Leu54 in Mdm2 is replaced with the larger Met53 in Mdmx, which makes the cavity of the p53-binding site in Mdmx narrower than that in Mdm2, thereby poorly accommodating a large molecule such as Nutlin-3a.[18] Although double inhibitors have also been developed for p53–Mdm2 and p53–Mdmx interactions,[19–21] few studies have investigated selective inhibitors for the p53–Mdmx interaction.[22,23] We recently discovered *o*-aminothiophenol derivatives with molecular weights of

* Corresponding authors. Tel./fax: +81 753412068 (S.U.); tel.: +81 335422511; fax: +81 335422530 (M.E.).
E-mail addresses: suesato@gaia.eonet.ne.jp, uesato@kansai-u.ac.jp (S. Uesato), menari@ncc.go.jp (M. Enari).

http://dx.doi.org/10.1016/j.bmc.2016.03.021
0968-0896/

200–300 in our protein–protein interaction (PPI)-inhibitor library.[24,25]

In the present study, we demonstrated that K-178 (**1c**) increased the expression of p53 as well as its downstream genes p21 and Mdm2 in IMR32 and MCF-7 cells with wild-type p53 and overexpressing Mdmx. Furthermore, K-178 (**1c**) dose-dependently suppressed the growth of cancer cells with wild-type p53 and Mdmx, whereas it only weakly influenced the growth of cancer cells with mutant p53. In order to analyze structure–activity relationships (SAR) in p53–Mdmx inhibitors, we further synthesized K-178 (**1c**)-related compounds with different substituents on *o*-aminothiophenol or *o*-aminophenol. The compounds obtained were subjected to a modified enzyme-linked immunosorbent assay (ELISA)[24,25] in order to examine the selectivity of the inhibition of p53–Mdm2 and p53–Mdmx interactions. The results obtained suggested that the *S*-isobutyryl-protected sulfide K-178 (**1c**) or K-181 (**3c**), after conversion to the corresponding monomeric sulfide **1b** or **3b**[26], preferentially interacted with p53–Mdmx over p-53–Mdm2 in the body. This bond may have triggered a deformation in the three-dimensional structure of p53 or Mdmx, leading to the dissociation of the two proteins. Oral administration experiments on K-178 (**1c**) in nude mice with human colon carcinoma (HCT116) tumor xenografts supported the results so far obtained.

2. Chemistry

Of the *N*,*N*′-di-carbamoyl disulfide derivatives **1a**–**5a**, **1a**,[27] **2a**[28] and **3a**[29] were known compounds. The derivatives **4a** and **5a** were synthesized by the reaction of 2,2′dithioaniline with 4-chlorobenzoyl chloride and 6-chloronicotinoyl chloride in the presence of *N*,*N*-diisopropylethylamine and *N*,*N*-4-dimethylaminopyridine, respectively (Scheme 1). The *N*,*S*-diisobutyryl- and *N*,*O*-diisobutyryl-substituted monomers **1c** and **1e** were prepared by the reaction of *o*-aminothiophenol and *o*-aminophenol with isobutyryl chloride and pyridine (Py), respectively. The other *S*-isobutyryl-protected monomer **3c** was synthesized starting from the disulfide **3a** via the corresponding sulfide **3b**. Thus, **3a** was reduced with $NaBH_4$ to give **3b**, which was treated with isobutyryl chloride in the typical manner to give **3c**. The sulfides **4b** and **5b** were prepared by the reduction of the disulfides **4b** and **5a** with $NaBH_4$ and PPh_3, respectively, whereas **1b** and **1d** were obtained by the alkaline hydrolysis of **1c** and **1e**, respectively.

3. Determination of inhibitory activities of *o*-aminothiophenol derivatives against the p53–Mdm2 or p53–Mdmx interaction using the modified ELISA

The *o*-aminothiophenols were subjected to the modified ELISA[24,25] in order to determine their inhibitory activities against the complex of Flag-p53 with glutathione *S*-transferase (GST)–Mdm2 or GST–Mdmx.

As shown in Table 1, *S*-isobutyryl-protected sulfides **1c** and **3c** preferentially disrupted binding between p53 and Mdmx over that between p53 and Mdm2. Additionally, they practically did not inhibit binding between p53 and the other p53-binding partners, death-associated protein kinase 1 (DAPK1)[30] and peptidylprolyl isomerase D (PPID).[31] This was also the case for the *S*-isobutyryl-deprotected forms **1b**, **3b**, **4b**, and **5b**, except for **2b**. Furthermore, the replacement of a sulfur atom (in **1b** and **1c**) with an oxygen atom (in **1d** and **1e**) resulted in the loss of inhibitory activities for binding between p53 and Mdmx, suggesting that the SH group in **1b** and **3b** may have an important role in the disruption of p53–Mdmx binding.

4. Effects of *o*-aminothiophenol derivatives on cell growth in various cancer cells

As shown in Figure 1, the cell viabilities of human mammary adenocarcinoma (MCF-7), human lung adenocarcinoma (A427), and HCT116 cells, all with wild-type p53 and Mdmx, were decreased by increasing concentrations of K-178 (**1c**). In contrast, the cell viabilities of cancer cells with mutant p53 such as human epidermoid carcinoma (A431) cells and human breast carcinoma (MDA-MB-468) cells as well as normal human embryonic lung fibroblasts (TIG-7) cells only moderately declined. These results suggest that the K-178 (**1c**)-mediated activation of the p53 pathway plays a pivotal role in suppressing the growth of cancer cells. Since acyl-protected sulfides are known to be metabolized into free sulfides by intracellular esterases,[32] the *S*-isobutyryl-deprotected form **1b** of K-178 (**1c**) appears to inhibit the growth of cancer cells.

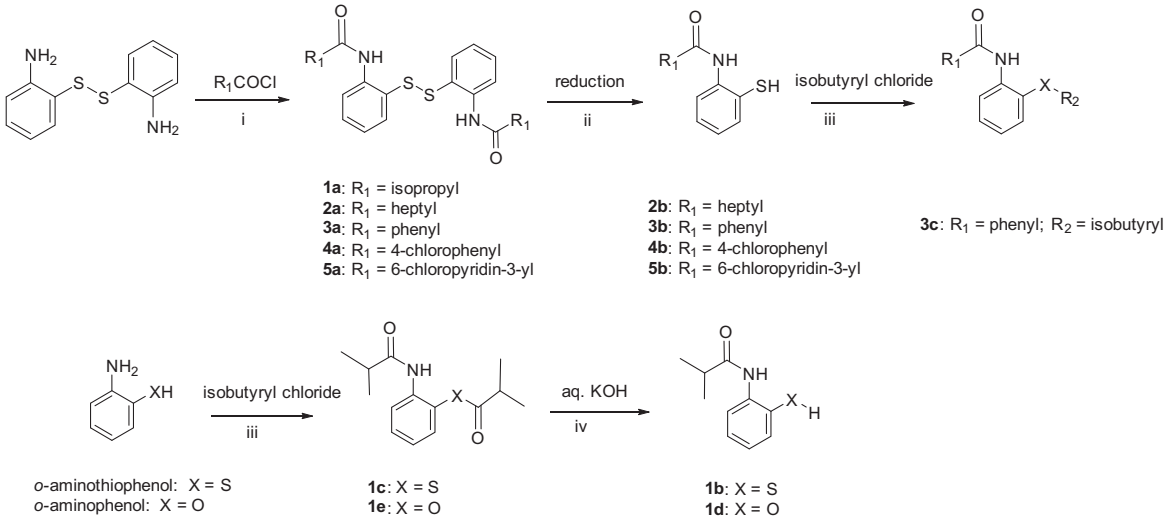

[a]Reagents and conditions: (i) *N*,*N*-diisopropylethylamine, CH_2Cl_2, rt (**4a**) or *N*,*N*-4-dimethylaminopyridine, DMF, rt (**5a**); (ii) $NaBH_4$, THF-EtOH, rt (**2b**),(**3b**),(**4b**) or PPh_3, THF, rt (**5b**); (iii) Py, CH_2Cl_2, rt; (iv) MeOH, rt.

Scheme 1. Synthesis of *o*-aminothiophenol derivatives.

Table 1
Inhibitory activities of *o*-aminothiophenol derivatives against the p53 and GST–protein interaction measured by the modified ELISA

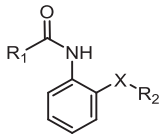

Compounds	R_1	X	R_2	Competitive inhibition (IC_{50}, μM)[a,b] of			
				p53–Mdm2	p53–Mdmx	p53–DAPK1	p53–PPID
1b	Isopropyl	S	H	>25	6.3	>25	>25
1c	Isopropyl	S	Isobutyryl	13.1	1.5	>25	>25
1d	Isopropyl	O	H	>25	>25	>25	>25
1e	Isopropyl	O	Isobutyryl	>25	>25	>25	>25
2b	Heptyl	S	H	>25	>25	>25	>25
3b	Phenyl	S	H	>25	7.2	>25	>25
3c	Phenyl	S	Isobutyryl	14.6	4.6	>25	>25
4b	4-Chlorophenyl	S	H	18.4	3.4	>25	>25
5b	6-Chloropyridin-3-yl	S	H	15.3	8.9	>25	>25
Nutlin-3a	—	—	—	0.5	8.2	>25	>25

[a] Inhibitory activities against the protein complexes were measured by the modified ELISA using Flag-p53 (10 mg) and GST–protein (1.5 mg).
[b] The compounds were subjected to the assay at concentrations of less than or equal to 25 mM owing to their limited solubilities.

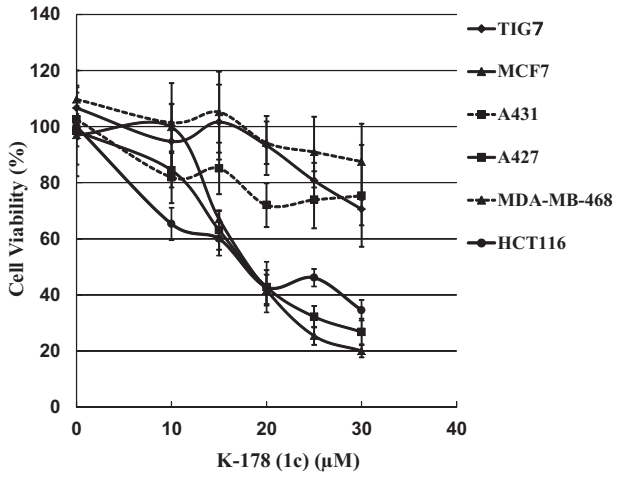

Figure 1. Effects of K-178 (**1c**) on growth in various cancer cells. Cells harboring wild-type or mutant p53 were incubated in the absence or presence of K-178 (**1c**) at the indicated concentrations. Cell viability was assayed 48 h after the treatment with K-178 (**1c**) by staining with crystal violet as described in Section 8. The following cells were used in this assay: MCF-7, A427, and HCT116 (Human cancer cells with wild-type p53); A431 and MDA-MB-468 (human cancer cells with mutant p53); TIG-7 (human normal cell).

5. Detection of p53, Mdm2, and p21 by a Western blot assay and localization of p53 by immunofluorescence microscopy

Western blot analyses showed that p53, Mdm2, and p21 levels were higher in MCF-7 cells treated with K-178 (**1c**) or Nutlin-3a than in control cells, and these increases occurred in a dose-dependent manner (Fig. 2A). These results suggest that the activation of p53 in cells treated with K-178 (**1c**) up-regulates the expression of its downstream genes such as p21 and Mdm2, as observed in cells treated with Nutlin-3a. The results of the immunofluorescence study confirmed that K178 (**1c**)- or Nutlin-3a-activated p53 accumulated in the nuclei of human neuroblastoma (IMR32) and MCF-7 cells (Fig. 2B).

6. Oral administration study on K-178 (1c) in nude mice with HCT116 xenografts

K-178 (**1c**) was orally administered to nude mice with HCT116 xenografts at a dose of 100 mg/kg or 150 mg/kg over 38 days according to the schedules indicated in Figure 3A. K-178 (**1c**) suppressed tumor growth in HCT116 xenografts to 49.0% and 36.6% that of the control at 100 mg/kg and 150 mg/kg, respectively, in 40 days. No weight losses were observed in either experiment (Fig. 3B).

A Western blotting analysis using proteins extracted from tumor masses showed that p53 and its downstream proteins Mdm2 and p21 were up-regulated, particularly in tumor masses in nude mice administered a dose of 150 mg/kg (Fig. 4), as observed in cells incubated with K-178 (**1c**) in vitro. Additionally, cleaved caspase 3, a marker of apoptosis, was markedly increased in tumors treated with **1c**. These results strongly suggest that the activation of p53 by K-178 (**1c**) occurs in vivo as detected by an in vitro assay. Furthermore, the treatment with K-178 (**1c**) increased the number of terminal transferase-mediated dUTP nick end-labeling (TUNEL)-positive cells in sections of tumor masses (Fig. 5A). The percentage of the apoptotic cell population was calculated by counting TUNEL-positive cells in microscopic fields, and the treatment with K-178 (**1c**) increased the number of TUNEL-positive cells in a dose-dependent manner (Fig. 5B).

7. Discussion and conclusion

We previously reported that the *S*-isobutyryl-protected *o*-aminothiophenol K179 disturbed, albeit weakly, binding between β-catenin and transcription factor 4 (TCF4) proteins.[33] In the present study, we found that the same series of compounds, K-178 (**1c**) and K-181 (**3c**), had the ability to inhibit binding between p53 and Mdmx. We prepared the related compounds **1b**, **1d**, **1e**, **2b**, **3b**, **4b**, and **5b** in order to analyze SAR as well as selectivity in the inhibition of binding between p53 and Mdm2 and between p53 and Mdmx using a modified ELISA. In the present study, not only the *S*-isobutyryl-deprotected sulfides **1b**, **3b**, **4b**, and **5b**, but also the *S*-isobutyryl-protected derivatives **1c** and **3c**, preferentially inhibited the p53–Mdmx interaction over the p53–Mdm2 interaction. Furthermore, inhibitory activity against the p53–Mdmx interaction was lost by replacing the sulfur atom in **1c** and **1b** by an oxygen atom in **1e** and **1d**. We speculate that **1b** or **3b** disrupted the p53–Mdmx interaction through disulfide-bond formation between the free thiol groups of **1b** or **3b** and Cys77 in Mdmx in the p53-binding domain. However, this speculation needs to be substantiated by spectroscopically detecting the presence of this disulfide bond. Furthermore, it is not clear why neither

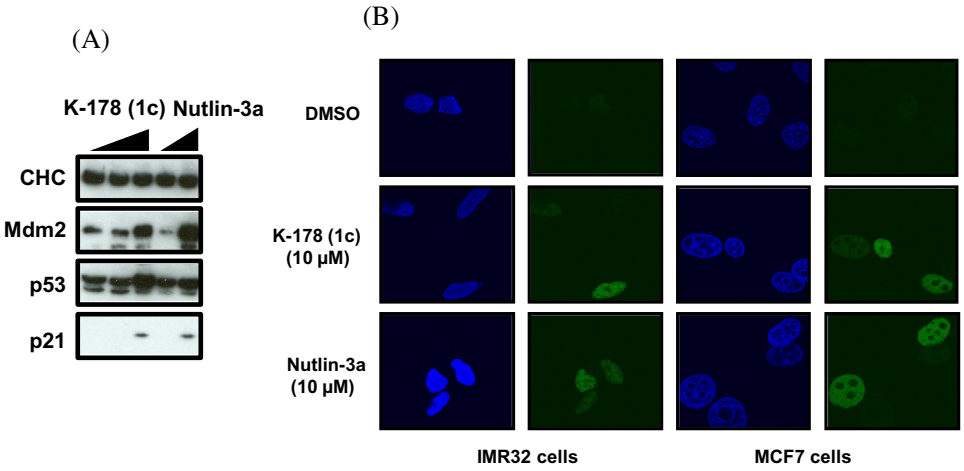

Figure 2. Detection of p53, Mdm2, and p21 by the Western blot assay and localization of p53 by immunofluorescence microscopy. (A) Cells were treated with K-178 (**1c**) for 24 h and expression levels of the indicated proteins in these cell lysates were determined by immunoblotting. (B) Cells were fixed with 3% paraformaldehyde 24 h after the treatment with K-178 (**1c**) and subjected to a confocal immunofluorescent analysis using the anti-p53 antibody (green). Nuclei were stained by DAPI (blue).

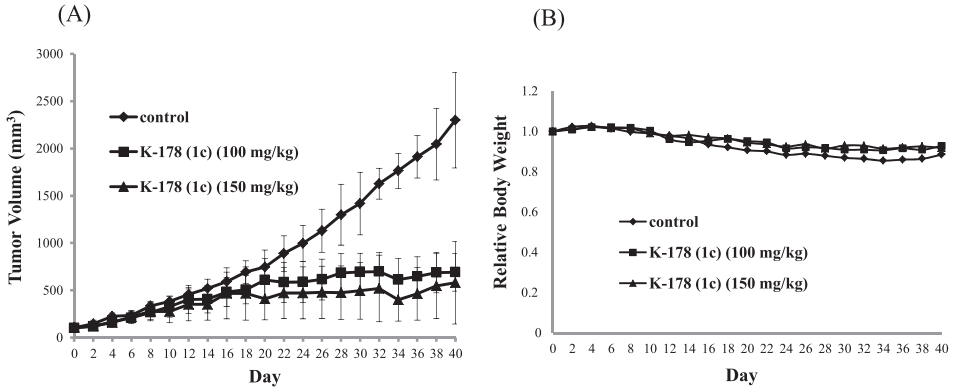

Figure 3. Oral administration study on K-178 (**1c**) in nude mice with HCT116 cell-inoculated xenografts. The effects of K-178 (**1c**) on tumor volume (A) as well as relative body weight (RBW) changes (B) at a dose of 100 mg or 150 mg/kg/day were examined as described in Section 8. K-178 (**1c**) was orally administered to mice every other day until day 38. Significant differences (p <0.05) were obtained for tumor volume with K-178 (**1c**) vs. the control as follows: K-178 (**1c**) (100 mg/kg) at all time points after day 22; K-178 (**1c**) (150 mg/kg) on days 4 and 14 as well as at all time points after day 20.

1b nor **3b** inhibited the binding of p53 to Cys76 in Mdm2. The reason for this may be interpreted in terms of differences in the steric bulkiness of the two C-terminal amino acids next to Cys between Mdmx and Mdm2 as follows. Mdmx has less hindered Gly78-Gly79 relative to Ser77 and Asn78 in Mdm2. Therefore, the sulfide **1b** or **3b** preferentially approaches from the less sterically hindered side to Cys77 in Mdmx. We also assume that the heptyl group in the sulfide **2b** is too bulky to inhibit the p53–Mdm2 and p53–Mdmx interactions.

In the present study, we demonstrated that *o*-aminothiophenol series compounds with molecular weights of 200–300 had the capabilities to inhibit the p53–Mdmx interaction. Based on the inhibitory effects of the same series of compound K-179 on β-catenin-TCF4 binding, the present series of compounds have the potential to inhibit a number of PPIs by changing substituents at the *N*-position or on a benzene ring. We expect *o*-aminothiophenol series compounds to provide a promising basis for the design and synthesis of new low-molecular-weight PPI inhibitors.

8. Experimental section

8.1. General

Melting points were determined on a Yanaco MP-500P micromelting point apparatus and were uncorrected. High-resolution mass spectra were measured on HPLC–ESI–LC–MS/MS (Prominance system, Shimadzu Co., Ltd and Q Exactive series, Thermo scientific Co., Ltd). ^{1}H NMR spectra were recorded on JEOL EX-400 (400 MHz) in $CDCl_3$, unless otherwise noted, as a solvent and tetramethylsilane as an internal standard. Analytical TLC was performed using Silica gel 60 F254 (Merck, 0.25 mm) glass plates. Column chromatography was performed using Silica Gel 60 (70–230 mesh ASTM) or flash chromatographs [Smart Flash EPCLC W-Prep 2XY (Yamazen) and Isolera One (Biotage)]. All solvents were dried over Na_2SO_4, and evaporated in vacuo. Bis(2-benzamidophenyl) disulfide (**3a**) was purchased from TCI Japan, Inc. The TUNEL assay reagent, DeadEnd™ Fluorometric TUNEL System, was obtained from Promega Corporation.

8.2. Synthesis

8.2.1. *S*-2-Isobutyramidophenyl 2-methylpropanethioate K-178 (1c)

Py (0.35 mL, 4.33 mmol) and isobutyryl chloride (0.43 mL, 4.04 mmol) were added to a solution of *o*-aminothiophenol (0.20 mL, 1.87 mmol) in CH_2Cl_2 (5 mL). After stirring at room temperature (RT) for 1 h, the reaction mixture was washed successively with 1% HCl, satd $NaHCO_3$, and brine. The organic layer was dried and concentrated to give a residue. Chromatography (*n*-hexane/EtOAc 5:1) over a silica gel and recrystallization from EtOH gave K-178 (**1c**) (466.6 mg, 1.76 mmol, yield 94.0%) as colorless needles.

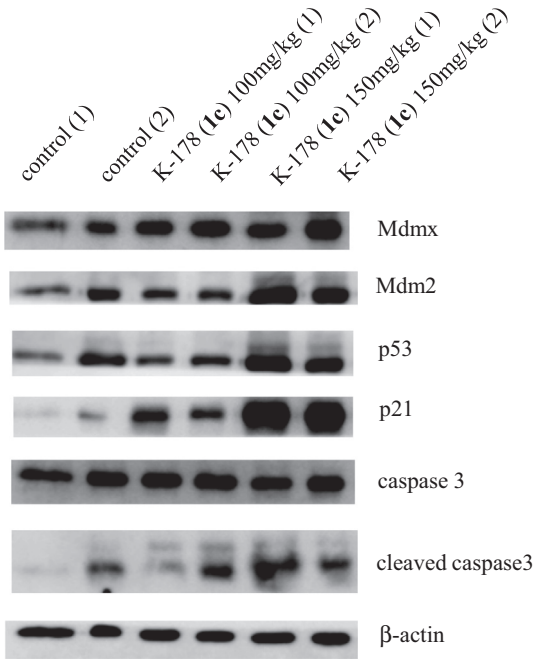

Figure 4. Western blot analysis of proteins derived from tumor masses. Tumor masses were removed from mice 40 days after initiating the administration of K-178 (**1c**), and expression levels of the indicated proteins in the lysates were determined by immunoblotting. The numbers (1) and (2) in parentheses indicate the numbering of arbitrary masses.

Mp 92–94 °C. ^{1}H NMR δ: 1.25 (6H, br d, J = 7.2 Hz, (CH_3)$_2$CH—), 1.30 (6H, br d, J = 7.2 Hz, (CH_3)$_2$CH—), 2.51 (1H, septet, J = 7.2 Hz, (CH_3)$_2CH$—), 2.94 (1H, septet, J = 7.2 Hz, (CH_3)$_2CH$—), 7.13 (1H, br t, J = 7.6 Hz, Ar-H), 7.38 (1H, br d, J = 7.6 Hz, Ar-H), 7.46 (1H, br t, J = 7.2 Hz, Ar-H), 7.77 (1H, br s, NH), 8.34 (1H, d, J = 7.6 Hz, Ar-H). HR-LC–ESI-MS m/z: $(M-H)^-$ calcd for $C_{14}H_{20}NO_2S$, 264.1058; found, 264.1065.

8.2.2. *N*-(2-Mercaptophenyl)isobutyramide (1b)

KOH (151 mg, 2.69 mmol) was added to a solution of **1c** (140 mg, 0.53 mmol) in THF (0.8 mL) and MeOH (0.8 mL). After stirring at rt for 4 h, the reaction mixture was diluted with water (10 mL) and concentrated to remove THF. The resulting aqueous solution was successively washed with *n*-hexane/EtOAc 1:1, adjusted to pH 4 with 1 M aq citric acid (2 mL), and extracted with $CHCl_3$. The $CHCl_3$ layer was dried and concentrated to yield a white solid, which was rinsed with *n*-hexane to afford **1b** (40.7 mg, 0.21 mmol, yield 39.5%).

Mp 83.3–87.0 °C. ^{1}H NMR δ : 1.31 (6H, d, J = 6.8 Hz, (CH_3)$_2$CH—), 2.62 (1H, septet, J = 6.8 Hz, (CH_3)$_2CH$—), 3.09 (1H, s, SH), 7.02 (1H, t, J = 8.0 Hz, Ar-H), 7.31 (1H, t, J = 8.0 Hz, Ar-H), 7.51 (1H, d, J = 8.0 Hz, Ar-H), 8.11 (1H, br s, NH), 8.30 (1H, d, J = 8.0 Hz, Ar-H). HR-LC–ESI-MS m/z: $(M-H)^-$ calcd for $C_{10}H_{12}NOS$, 194.0640; found 194.0637.

8.2.3. *N*-(2-Mercaptophenyl)octanamide (2b)

$NaBH_4$ (20.6 mg, 0.54 mmol) was added in one portion at 0 °C to a solution of *N*,*N*′-(disulfanediylbis(2,1-phenylene)dioctanamide (**2a**) (151 mg, 0.30 mmol) in THF (2.4 mL) and EtOH (0.6 mL). After stirring at rt for 3 h, 1 M aq NaOH (5 mL) and then 1 M aq citric acid (2 mL) was added to the reaction mixture, which was extracted with EtOAc. The EtOAc layer was dried and concentrated. The crude product was purified by flash column chromatography on a silica gel (EtOAc/*n*-hexane) to yield **2b** as a yellowish oil (3.9 mg, 0.016 mmol, yield 2.6%). ^{1}H NMR δ: 0.86–0.88 (3H, m, $CH_3(CH_2)_4CH_2$—), 1.27–1.31 (8H, m, $CH_3(CH_2)_4CH_2$—), 1.55–1.64 (1H, m, —CH_2CH_2CO), 1.86–1.95 (1H, m, —CH_2CH_2CO), 2.28 (1H, t, J = 7.6 Hz, —CH_2CH_2CO), 3.39 (1H, dd, J = 8.7, 6.0 Hz, —CH_2CH_2CO), 4.03 (1H, s, SH), 6.82 (1H, dd, J = 8.0, 1.1 Hz, Ar-H), 7.01 (1H, td, J = 7.6, 1.2 Hz, Ar-H), 7.17 (1H, td, J = 7.6, 1.4 Hz, Ar-H), 7.31–7.33 (1H, m, Ar-H), 8.07 (1H, s, NH). HR-LC–ESI-MS m/z: $(M-H)^-$ calcd for $C_{14}H_{20}NOS$, 250.1266; found 250.1272.

8.2.4. *N*-(2-mercaptophenyl)benzamide (3b)

To a solution of bis(2-benzamidophenyl)disulfide (**3a**) (140 mg, 0.31 mmol) in THF (2.4 mL) and EtOH (0.8 mL) was added $NaBH_4$ (12 mg, 0.32 mmol) in one portion. After stirring at rt for 1.5 h, 2 M aq NaOH (10 mL) was added to the reaction mixture, which was then washed with *n*-hexane/EtOAc 2:1. The water layer was successively adjusted to pH 4 with 1 M aq citric acid (10 mL) and extracted with EtOAc. The EtOAc layer were dried and concentrated to yield a white solid. The resulting solid was washed with Et_2O to afford **3b** (15 mg, 0.065 mmol, yield 11%). Mp 98.0–101.3 °C. ^{1}H NMR δ: 3.17 (s, 1H, SH), 7.08 (1H, td, J = 7.4, 1.2 Hz, Ar-H), 7.39 (1H, t, J = 7.8 Hz, Ar-H), 7.61-7.51 (4H, m, Ar-H×4), 7.98–7.96 (2H, m, Ar-H$_2$), 8.48 (1H, d, J = 8.4 Hz, Ar-H), 8.94 (1H, br s, NH). HR-LC–ESI-MS m/z: $(M-H)^-$ calcd for $C_{13}H_{10}NOS$, 228.0483; found 228.0485.

8.2.5. *S*-2-Benzamidophenyl 2-methylpropanethioate K-181 (3c)

$NaBH_4$ (113.5 mg, 3.00 mmol) was added under ice-cooling to a solution of bis(2-benzoylaminophenyl)disulfide (**3a**) (456.6 mg,

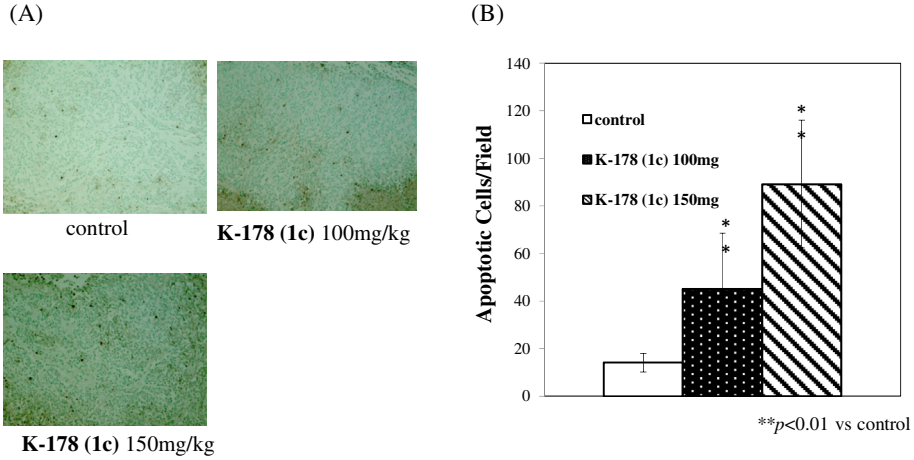

Figure 5. Detection of TUNEL-positive cells in sections prepared from tumor masses. Tumor masses were treated as indicated in Section 8. (A) TUNEL-positive cells (brown in color) were visualized with fluorescent microscopy according to the procedure indicated in Section 8. (B) TUNEL-positive cells as a percentage of all cells in the microscopic field were determined by examining eight fields per view at ×20 magnification and then expressed in the form of bar graphs.

1.00 mmol) in THF (4 mL) and EtOH (20 mL). After stirring at rt for 2 h, the reaction mixture was quenched by a few drops of acetic acid and concentrated. The residue was dissolved in EtOAc, and the solution was washed with water. The organic layer was dried and concentrated to give a yellowish solid. This substance, without purification, was, in turn, subjected to isobutyrylation with isobutyryl chloride (0.422 mL, 4.00 mmol) and Py (0.322 mL, 3.98 mmol) in CH_2Cl_2 (5 mL) in the same manner as that described for the preparation of **2c**, giving **3c** (205.0 mg, 0.68 mmol, yield 34.2%).

Mp 104.6–105.7 °C. ^{1}H NMR (DMSO-d_6) δ: 1.09 (6H, d, J = 6.8 Hz, $(CH_3)_2CH$—), 2.65 (1H, septet, J = 6.8 Hz, $(CH_3)_2CH$—), 7.33 (1H, t, J = 8.0 Hz, Ar-H), 7.47–7.54 (4H, m, Ar-H_4), 7.58 (1H, d, J = 7.2 Hz, Ar-H), 7.62 (1H, d, J = 7.6 Hz, Ar-H), 7.92 (2H, d, A_2 of A_2B_2, J = 7.6 Hz, Ar-H_2), 9.93 (1H, br s, NH). HR-FAB-MS m/z: $(M+H)^+$ calcd for $C_{22}H_{18}N_3O_9$, 300.1059; found, 300.1054.

8.2.6. 2-Isobutyramidophenyl isobutyrate (1e)

Py (2.21 mL, 27.3 mmol) and isobutyryl chloride (2.90 mL, 27.5 mmol) were added to a solution of *o*-aminophenol (1.00 g, 9.16 mmol) in CH_2Cl_2 (5 mL). After stirring at rt for 30 min, the reaction mixture was washed successively with 1% HCl, satd $NaHCO_3$, and brine. The organic layer was dried and concentrated to give a solid. Recrystallization from $CHCl_3$ and *n*-hexane gave **1e** (1.65 g, 6.62 mmol, yield 72.2%) as colorless needles.

Mp 88.5–90.6 °C. ^{1}H NMR δ: 1.25 (6H, d, J = 6.8 Hz, $(CH_3)_2CH$—), 1.37 (6H, J = 6.8 Hz, $(CH_3)_2CH$—), 2.51 (1H, septet, J = 6.8 Hz, $(CH_3)_2CH$—), 2.94 (1H, septet, J = 6.8 Hz, $(CH_3)_2CH$—), 7.11–7.30 (3H, m, Ar-H_3). HR-LC–ESI-MS m/z: $(M-H)^-$ calcd for $C_{14}H_{18}NO_3$, 248.1287; found 248.1292.

8.2.7. *N*-(2-Hydroxyphenyl)isobutyramide (1d)

A total of 5 N aq KOH (1.21 mL, 6.03 mmol) was added to a solution of **1e** (500.0 mg, 1.70 mmol) in EtOH (10 mL). The progress of the reaction was monitored by TLC. When the reaction ceased, the reaction mixture was adjusted to pH 6.0 with 1 N HCl and concentrated. The residue was dissolved in EtOAc and washed successively with satd $NaHCO_3$ and brine. The organic layer was dried and concentrated to give **1d** (169.1 mg, 0.94 mmol, yield 55.5%) as colorless needles. Mp 107.4–109.2 °C. ^{1}H NMR δ: 1.31 (6H, d, J = 7.2 Hz, $(CH_3)_2CH$—), 2.65 (1H, septet, J = 6.8 Hz, $(CH_3)_2CH$—), 6.86 (1H, t, J = 7.2 Hz, Ar-H), 6.97 (1H, d, J = 8.0 Hz, Ar-H), 7.02 (1H, d, J = 8.0 Hz, Ar-H), 7.13 (1H, t, J = 7.2 Hz, Ar-H), 7.40 (1H, br s, OH), 8.86 (1H, br s, NH). HR-LC–ESI-MS m/z: $(M-H)^-$ calcd for $C_{10}H_{12}NO_2$, 178.0868; found 178.0861.

8.2.8. *N,N′*-(Disulfanediylbis(2,1-phenylene))bis(4-chlorobenzamide) (4a)

4-Chlorobenzoyl chloride (1.08 mL, 8.46 mmol) was added to a solution of 2,2′-dithioaniline (1000 mg, 4.03 mmol) in *N,N*-diisopropylethylamine (1.75 mL, 10.1 mmol) and CH_2Cl_2 (13.4 mL). After stirring at rt for 2 h, the resulting white precipitate was collected and washed with water (20 mL). The resulting solid was dried at rt to afford **4a** as a white solid (1780 mg, 3.40 mmol, yield 84%). Mp 178.0–178.8 °C. ^{1}H NMR δ: 6.97 (4H, td, J = 7.6, 1.2 Hz, Ar-H_2×2), 7.30 (2H, td, J = 8.6, 1.0 Hz, Ar-H_2×2), 7.41, 7.57 (8H, A_2B_2, J = 8.4 Hz, Ar-H_4×2), 7.46 (4H, dd, J = 7.8, 1.8 Hz, Ar-H_2×2), 8.43 (4H, dd, J = 8.0, 1.0 Hz, —NH×2). HR-LC-ESI-MS m/z: $(M-H)^-$ calcd for $C_{26}H_{18}Cl_2N_2O_2S_2$, 523.0109; found 523.0121.

8.2.9. 4-Chloro-*N*-(2-mercaptophenyl)benzamide (4b)

$NaBH_4$ (34 mg, 0.90 mmol) was added in one portion to a solution of **4a** (262 mg, 0.50 mmol) in THF (4.0 mL) and EtOH (1.0 mL). After stirring at rt for 8 h, 1 M aq NaOH (10 mL) was added to the reaction mixture, which was then washed with *n*-hexane/EtOAc 2:1. The water layer was successively adjusted to pH 4 with 1 M aq citric acid (4 mL) and extracted with $CHCl_3$. The $CHCl_3$ layer were dried and concentrated to yield a white solid, which was washed with *n*-hexane to afford **4b** (178 mg, 0.67 mmol, yield 68%) as a white solid.

Mp 110.1–113.6 °C.^{1}H NMR δ : 3.17 (1H, s) 7.09 (1H, t, J = 8.0 Hz, Ar-H) 7.39 (1H, t, J = 8.0 Hz, Ar-H) 7.50 (2H, td, J = 2.4, 8.8 Hz, Ar-H_2), 7.58 (1H, d, J = 8.0 Hz, Ar-H), 7.90 (2H, td, J = 2.4, 8.8 Hz, Ar-H_2), 8.44 (1H, d, J = 8.0 Hz, Ar-H), 8.90 (1H, br s, NH). HR-LC–ESI-MS m/z: $(M-H)^-$ calcd for $C_{13}H_8ClN_2OS$, 263.0046; found 263.0047.

8.2.10. *N,N′*-(Disulfanediylbis(2,1-phenylene))bis(6-chloronicotinamide) (5a)

N,N-4-Dimethylaminopyridine (0.590 mL, 4.82 mmol) and 6-chloronicotinoyl chloride (850 mg, 4.82 mmol) were added to a solution of 2,2′-dithiodianiline (500 mg, 2.01 mmol) in *N,N*-dimethylformamide (DMF) (10 mL). After stirring at rt for 9 h, DMF was removed and washed successively with water and EtOH. Recrystallization from $CHCl_3$ gave **5a** (600 mg, 1.14 mmol, yield 56.6%) as colorless needles.

Mp 216.1–218.0 °C. ^{1}H NMR δ: 7.01 (2H, td, J = 7.7, 1.6 Hz, Ar-H×2), 7.27 (2H, td, J = 8.0, 1.4 Hz, Ar-H×2), 7.44 (2H, dd, J = 8.4, 0.8 Hz, Ar-H×2), 7.53 (2H, dd, J = 7.8, 1.4 Hz, Ar-H×2), 7.90 (2H, dd, J = 8.4, 2.4 Hz, Ar-H×2), 8.34 (2H, dd, J = 8.4, 1.2 Hz, Ar-H×2), 8.63 (2H, br d, J = 2.4 Hz, Ar-H×2), 8.77 (2H, br s, NH×2). HR-ESI-MS m/z: $(M+H)^+$ calcd for $C_{24}H_{17}Cl_2N_4O_2S_2$, 527.0171; found, 527.0169.

8.2.11. 6-Chloro-*N*-(2-mercaptophenyl)nicotinamide (5b)

PPh_3 (102 mg, 0.39 mmol) was added in one portion at 0 °C to a solution of **5a** (102 mg, 0.19 mmol) in THF (1.9 mL). After stirring at rt for 3 h, the reaction mixture was concentrated in vacuo to give a crude product, which was purified by flash column chromatography on a silica gel (EtOAc/*n*-hexane) to yield **5b** as a white solid (12.9 mg, 0.049 mmol, yield 12.9%). Mp 135.1–136.4 °C. ^{1}H NMR δ: 3.75 (1H, s, SH), 7.26–7.28 (1H, m, Ar-H), 7.43–7.56 (3H, m, Ar-H_3), 7.95 (1H, d, J = 7.8 Hz, Ar-H), 8.11 (1H, d, J = 8.0 Hz, Ar-H), 8.36 (1H, dd, J = 8.3, 2.7 Hz, Ar-H), 9.07 (1H, s, NH). HR–ESI-MS m/z: $(M-H)^-$ calcd for $C_{13}H_9ClNOS$, 262.0093; found 262.0100.

8.3. Cell lines, cultures, and antibodies

HCT116 (wild-type p53), TIG7 (wild-type p53), MCF-7 (wild-type p53), A427 (wild-type p53), A431 (mutant p53), and MDA-MB-468 (mutant p53) cell lines were purchased from the American Type Culture Collection (ATCC). IMR32 (wild-type p53) was a gift from Dr. Nakagawara (Saga-ken Medical Centre Koseikan). HCT116 cells were cultured in McCoy's medium (GIBCO), supplemented with 10%fetal bovine serum (FBS) (Biowest or GIBCO), 50 μg/mL penicillin G, and 50 μg/mL streptomycin sulfate (GIBCO) in a 5% CO_2 and 95% air atmosphere at 37 °C. TIG-7 cells were cultured in Dulbecco's Modified Eagle Medium (Sigma–Aldrich) supplemented with 10% FBS, 50 μg/mL penicillin G, and 50 μg/mL streptomycin sulfate (GIBCO) in a 5% CO_2 and 95% air atmosphere at 37 °C. Other cells were cultured in RPMI-1640 (Sigma–Aldrich) supplemented with 10% FBS, 50 μg/mL penicillin G, and 50 μg/mL streptomycin sulfate (GIBCO) in a 5% CO_2 and 95% air atmosphere at 37 °C. Trypsin was purchased from GIBCO, and CELLBANKER **2** was from Nippon Zenyaku Kogyo Co., Ltd. The anti-actin antibody was purchased from Sigma–Aldrich. The anti-p53 antibody was from Santa Cruz Biotechnology, antibodies specific to Mdm2 were from Abcam and Merck Millipore (Calbiochem), and the anti-Mdmx antibody was from Abcam. The anti-p21 antibodies were from BioLegend and Abcam, and the anti-caspase 3 antibody was from BioLegend. The antibody to cleaved caspase 3 (Asp175) was from Cell Signaling Technology. ECL™ Anti-Rabbit IgG, Horseradish Peroxidase-linked whole antibody, ECL™ Anti-mouse IgG,

Horseradish Peroxidase-linked whole antibody, and ECL™ Prime Western Blotting Detection Reagent were from GE Healthcare. SuperSignal West Femto Chemiluminescent Substrate was from Thermo SCIENTIFIC.

8.4. Animals

Female BALB/c-nu.nu nude mice (5 weeks old) were purchased from Japan SLC Inc. Animals were housed and experiments were performed according to the guidelines stipulated by the Osaka University of Pharmaceutical Sciences Animal Care and Use Committee. Mice were used at 6 weeks of age.

8.5. Cell viability assays using crystal violet

Cells were plated at a density of 2×10^4 cells/well on 24-well microtiter plates. After incubating in an atmosphere of 5% CO_2 and 95% air at 37 °C for 24 h, cells were grown in the presence of serially diluted samples for 48 h and then stained for 15 min with a crystal violet solution (0.75% crystal violet, 0.25% NaCl, 1.75% formaldehyde, 50% EtOH, and 47.25% MilliQ). The absorbance of the solutions was measured spectrophotometrically at 600 nm using a SH-1000 Microplate Reader (Corona Electric Co., Ltd), and cell viability was assessed. Cell viability (%) relative to the control at each concentration point (0, 10, 15, 20, 25, or 30 μM) was calculated by the number of tested cells/number of control cells × 100.

8.6. In vivo antitumor tests

HCT116 cells (1.5×10^6/100 μL of Matrigel™ (BD Biosciences) were injected subcutaneously into the backs of nude mice (6 weeks old). K-178 (**1c**) (2.0 or 3.0 mg/200 μL) ($n = 6$ or 9) as well as vehicle (0.1% Tween 80, 200 μL) ($n = 7$) were administered orally to nude mice with tumors (tumor size: 70–143 mm^3) every other day until day 38. Tumor length and width as well as body weight were monitored. Tumor volume (mm^3) was calculated by measuring tumor length and width (in mm) as described.[34] Antitumor activity was expressed as the percentage of mean tumor volumes for treated mice to mean tumor volumes for control mice. At day 40, the cervical spine was dislocated and the chest was opened. Tumor masses were removed and weighed as they were.

8.7. Western blot analysis

Cells were plated on 60-mm diameter dishes (1.0×10^6/dish) in medium supplemented with FBS, penicillin (20 U/mL), and streptomycin (20 mg/mL). After being incubated for 24 h, the cells were washed twice with medium (1 mL each). After the addition of medium (5 mL), the culture was incubated for another 24 h and then treated with the tested compound, Nutrin-3a or control (0.1% DMSO) for 24 or 48 h. Medium was discarded, and floating and adhered cells were washed with PBS (2 × 1 mL), scraped, and homogenized for 1 min in 400 μL of lysis buffer (5 mM Tris–HCl buffer saline, 15 mM NaCl, 0.2 mM $MgCl_2$, 0.1 mM EDTA, 0.1 mM EGTA, 0.01% NP-40, 1 mM Na_3VO_4, 10 mM NaF, 1 mM DTT, and 1 mM PMSF) containing proteinase inhibitor cocktail (Nacalai Tesque) at 0 °C. Tumor masses were also frozen with liquid nitrogen and immediately ground into pieces. The resulting powder was suspended in the above-described lysis buffer. The lysates from cells or tumor masses were centrifuged at 15,000×*g* at 4 °C for 15 min. Protein concentrations were determined with a BCA protein assay kit (Thermo Fisher Scientific). An equal amount (10 μg) of protein was then resolved by SDS–PAGE and transferred to a PVDF membrane (Millipore). Blots (1× Tris–HCl buffer saline, 5% nonfat milk, and 0.05% Tween 20) were probed with an antibody specific to each protein. Primary monoclonal antibodies against the following proteins were used: β-actin, p53, Mdm2, Mdmx, p21, and cleaved caspase 3 at a 1:1000 dilution; full-length caspase 3 at a 3:1000 dilution). Secondary antibodies conjugated to horseradish peroxidase (at a 1:1000–2000 dilution) (GE Healthcare, UK) were used, and blots were further incubated with ECL™ Prime Western Blotting Detection Reagent (GE Healthcare) or SuperSignal® West Femto Maximum Sensitivity Substrate (Thermo Fisher Scientific). Immunoreactive proteins were detected using ECL chemiluminescence (Image Quant LAS 3000 detection system) (GE Healthcare).

8.8. Detection of apoptotic cells by the TUNEL method

The TUNEL assay to detect apoptosis in the tumor masses was outsourced to Applied Medical Research Co., Ltd, Japan. Tumor masses were collected and fixed in 4% paraformaldehyde overnight, dehydrated, and embedded in paraffin the next day. Tumor sections were deparaffinized, then rehydrated and treated with an Apop Tag Peroxidase In Situ Apoptosis Detection Kit (Millipore) according to the manufacturer's protocol. TUNEL-positive cells as a percentage of all cells in a microscopic field were determined by examining eight fields of a view at ×20 magnification with a Keyence BZ-9000 microscope.

8.9. Immunofluorescence

HCT116. or MCF-7 cells were seeded at a concentration of 3.0×10^4/mL in a 4-well chamber slide with 0.4 mL medium per well and incubated for 24 h. After the addition of each test sample (10 μM), the incubation was continued for a further 24 h. Cells were fixed with 3% paraformaldehyde in PBS at 25 °C for 30 min and then permeabilized with 0.05% Triton X-100 in PBS at 25 °C for 5 min. The chamber slide was rinsed with PBS (200 μL × 4), and cells were blocked with 3% BSA in PBS for 10 min. Cells were then exposed to a 1:50 dilution of the p53 Antibody (FL-393) (Santa Cruz) overnight at 4 °C followed by a treatment with a 1:200 dilution of the goat anti-mouse IgG (H+L) secondary antibody conjugated to Alexa Fluor® 488 (Molecular Probes) containing propidium iodide (Dojindo, Japan) (35 μg/mL) at RT for 30 min. PBS containing 3% BSA was used to dilute antibodies. After removal of the PBS solution containing the unbound secondary antibody, a few drops of DAPI (Dojindo, Japan) and PBS (500 μL) were added successively to each well. Cells in each well were viewed under fluorescence microscopy (magnification ×40) (Biorevo, Keyence, Japan).

8.10. Preparation of GST–Mdm2, GST–Mdmx, GST–DAPK1, GST–PPID, and Flag-p53

GST–Mdm2, GST–Mdmx, GST–DAPK1, GST–PPID, and Flag-p53 were prepared in an analogous manner to the reported procedures.[24,25] Thus, GST–Mdm2, GST–Mdmx, GST–DAPK1, GST–PPID, and GST–Flag-p53 constructs in pGEX6P-1 vectors (GE Healthcare) were transformed into *Escherichia coli* BL21 (DE3) (Novagen) by the heat shock method. Cells were grown at 37 °C overnight on LB/agar (Merck) containing 100 μg/ml ampicillin. Cells were then transferred into LB liquid medium containing 100 μg/ml ampicillin, suspended at 37 °C until OD600 reached to 0.6, and induced with 0.1 mM IPTG (Nacalai Tesque) at 30 °C for 3 h. The bacteria pellet was collected, resuspended and sonicated in PBST (1× PBS containing 0.1% Tween 20). The lysates were centrifuged at 7000 rpm for 10 min. The supernatants were collected and dialyzed against 20 mM PBS, and the GST fusion proteins were purified by an ÄKTA Explorer system with the pre-loaded GSTrap column (GE Healthcare) using an elution buffer [10 mM glutathione–20 mM PBS (pH 8.2)]. GST–Flag-p53 was treated with Turbo3C protease

(Nacalai Tesque), and the resultant Flag-p53 was purified by the ÄKTA Explorer system in the typical manner.

8.11. Measurement of the inhibition of *o*-aminothiophenols using the modified ELISA

In the preparation of the ELISA system, glutathione-coated plates [8-well Strip (Thermo Scientific)] were saturated with 1× PBS containing 1% skim milk (Nacalai Tesque) at rt for 1 h. After removal of the buffer, a solution of the GST-fused protein in 1× PBS containing 1% skim milk was immobilized on the glutathione-coated plates at RT for 1 h. The plates were then washed with PBST and incubated with FLAG-p53. The *o*-aminothiophenols **1b**–**1e**, **2b**, **3b**–**3c**, **4b**, and **5b**, as well as the positive control Nutlin-3a, were added to these plates. After being incubated for 1 h, the plates were washed with PBST and incubated with the anti-Flag antibody (at a 1:10,000 dilution with 1× PBS containing 1% skim milk) at rt for 1 h. After washing with PBST to remove the buffer, absorbance at 492 nm was measured by a microplate reader (Model 680 XR, Bio-Rad) using a HRP-peroxidase kit (Sumitomo Bakelite) as reported previously.[24,25] The half maximal inhibitory concentrations (IC_{50}) of the interaction between Flag-p53 and GST–protein were calculated using data obtained at a concentration of 0.25 μM, 2.5 μM, or 25.0 M.

8.12. Statistical analysis

At each time point, the heterogeneity of results across the studies was tested using the Cochran Q test. The significance of differences in the effects of drugs vs. the control was analyzed with the Student's *t*-test.

Acknowledgments

We are very grateful to Professor Masahiko Taniguchi and Associate Professor Makio Shibano (Osaka University of Pharmaceutical Sciences) for their kind support with the in vivo experiments. We also thank Dr. Nakagawara for providing IMR32 cells. Part of this work was supported by the following grants: Project for the Development of Innovative Research on Cancer Therapeutics (P-DIRECT) from Ministry of Education, Culture, Sports, Science, and Technology – Japan, Applied Research for Innovative Treatment of Cancer from Ministry of Health, Labour and Welfare – Japan (M.E.), Grant-in-Aid for Scientific Research (B) (24390222) from Ministry of Education, Culture, Sports, Science, and Technology – Japan (T.S.) and MEXT – Supported Program for the Strategic Research Foundation at Private Universities (2013–2017) – Japan (S.U.).

Supplementary data

Supplementary data associated with this article can be found, in the online version, at http://dx.doi.org/10.1016/j.bmc.2016.03.021.

References and notes

1. Ryan, K. M.; Phillips, A. C.; Vousden, K. H. *Curr. Opin. Cell Biol.* **2001**, *13*, 332.
2. Evan, G. I.; Vousden, K. H. *Nature* **2001**, *411*, 342.
3. Ingrid Herr, I.; Debatin, K. M. *Blood* **2001**, *98*, 2603.
4. Haupt, S.; Berger, M.; Goldberg, Z.; Haupt, Y. *J. Cell Sci.* **2003**, *116*, 4077.
5. Beckerman, R.; Prives, C. *Cold Spring Harb. Perspect. Biol.* **2010**, *2*, a000935. http://dx.doi.org/10.1101/cshperspect.a000935.
6. Brooks, C. L.; Gu, W. *Mol. Cell* **2006**, *21*, 307.
7. Yamasaki, S.; Yagishita, N.; Sasaki, T.; Nakazawa, M.; Kato, Y.; Yamadera, T.; Bae, E.; Toriyama, S.; Ikeda, R.; Zhang, L.; Fujitani, K.; Yoo, E.; Tsuchimochi, K.; Ohta, T.; Araya, N.; Fujita, H.; Aratani, S.; Eguchi, K.; Komiya, S.; Maruyama, I.; Higashi, N.; Sato, M.; Senoo, H.; Ochi, T.; Yokoyama, S.; Amano, T.; Kim, J.; Gay, S.; Fukamizu, A.; Nishioka, K.; Tanaka, K.; Nakajima1, T. *The EMBO Journal* **2007**, *26*, 113.
8. Hock, A. K.; Vousden, K. H. *Biochim. Biophys. Acta* **2014**, *137*, 1843.
9. Wade, M.; Li, Y. C.; Wahl, G. M. *Nat. Rev. Cancer* **2013**, *13*, 83.
10. Wang, X.; Jiang *FEBS Lett.* **2012**, *586*, 1390.
11. Zhao, Y.; Bernard, D.; Wang, S. *BioDiscovery* **2013**, *8*, 4.
12. Mohammad, R. M.; Wu, J.; Azmi, A. S.; Aboukamee, A.; Sosin, A.; Wu, S.; Yang, D.; Wang, S.; Al-Katib, A. M. *Mol. Cancer* **2009**, *8*, 115.
13. Ding, Q.; Zhang, Z.; Liu, J.-J.; Jiang, N.; Zhang, J.; Ross, T. M.; Chu, X.-J.; Bartkovitz, D.; Podlaski, F.; Janson, C.; Tovar, C.; Filipovic, Z. M.; Higgins, B.; Glenn, K.; Packman, K.; Vassilev, L. T.; Graves, B. *J. Med. Chem.* **2013**, *56*, 5979.
14. Wang, W.; Qin, J.-J.; Voruganti, S.; Srivenugopal, K. S.; Nag, S.; Patil, S.; Sharma, H.; Wang, M.-H.; Wang, H.; Buolamwini, J. K.; Zhang, R. *Nat. Commun.* **2014**, *5*, 5086. http://dx.doi.org/10.1038/ncomms6086.
15. Kumar, S. K.; Hager, E.; Pettit, C.; Gurulingappa, H.; Davidson, N. E.; Khan, S. R. *J. Med. Chem.* **2003**, *46*, 2813.
16. Vassilev, L. T.; Vu, B. T.; Graves, B.; Carvajal, D.; Podlaski, F.; Filipovic, Z.; Kong, N.; Kammlott, U.; Lukacs, C.; Klein, C.; Fotouhi, N.; Liu, E. A. *Science* **2004**, *303*, 844.
17. Hu, B.; Gilkes, D. M.; Farooqi, B.; Sebti, S. M.; Chen, J. *J. Biol. Chem.* **2006**, *281*, 33030.
18. Joseph, T. L.; Madhumalar, A.; Brown, C. J.; Lane, D. P.; Verma, C. *Cell Cycle* **2010**, *9*, 1167.
19. Dömling, A. *Curr. Opin. Chem. Biol.* **2008**, *12*, 281.
20. Phan, J.; Li, Z.; Kasprzak, A.; Li, B.; Sebti, S.; Guida, W.; Schönbrunn, E.; Chen, J. *J. Biol. Chem.* **2010**, *285*, 2174.
21. Popowicz, G. M.; Dömling, A.; Holak *Angew. Chem., Int. Ed.* **2011**, *50*, 2680.
22. Reed, D.; Shen, Y.; Shelat, A. A.; Arnold, L. A.; Ferreira, A. M.; Zhu, F.; Mills, N.; Smithson, D. C.; Regni, C. A.; Bashford, D.; Cicero, S. A.; Schulman, B. A.; Jochemsen, A. G.; Guy, R. K.; Dyer, M. A. *J. Biol. Chem.* **2010**, *285*, 10786.
23. Zhang, Q.; Zeng, S. X.; Lu, H. *Sub-Cell Biochem.* **2014**, *85*, 281.
24. Enari, M.; Kawaratani, Y.; Uesato, S.; Yokota, 69th Annual Meeting of the Japanese Cancer Association, 2010, Osaka.
25. Enari, M.; Uesato, S. JP Patent Application No. 2011-178704.
26. Ito, A. *Yakugaku Zasshi* **1962**, *82*, 875.
27. Davis, A. R. *Ind. Eng. Chem.* **1947**, *39*, 94.
28. Shinkai, H.; Maeda, K.; Yamasaki, T.; Okamoto, H.; Uchida, I. *J. Med. Chem.* **2010**, *43*, 3566.
29. Bogert, M. T.; Snell, F. D. J. *Amer. Chem. Soc.* **1924**, *46*, 1308.
30. Pei, L.; Shang, Y.; Jin, H.; Wang, S.; Wei, N.; Yan, H.; Wu, Y.; Yao, C.; Wang, X.; Zhu, L. Q.; Lu, Y. *J. Neurosci.* **2014**, *34*, 6546.
31. Zhao, L. P.; Ji, C.; Lu, P. H.; Li, C.; Xu, B.; Gao, H. *Neurochem. Res.* **2013**, *38*, 705.
32. Baud, M. G. J.; Leiser, T.; Petrucci, V.; Gunaratnam, M.; Neidle, S.; Meyer-Almes, F.-J.; Fuchter, M. J. *Beilstein J. Org. Chem.* **2013**, *9*, 81.
33. Yamakawa, S.; Demizu, A.; Kawaratani, Y.; Nagaoka, Y.; Terada, Y.; Maruyama, S.; Uesato, S. *Biol. Pharm. Bull.* **2008**, *31*, 916.
34. Komatsu, Y.; Tsukamoto, M.; Kato, T.; Nishino, N.; Sato, S.; Yamori, T.; Tsuruo, T.; Furumai, R.; Yoshida, M.; Horinouchi, S.; Hayashi, H. *Cancer Res.* **2001**, *61*, 4459.